Technical Memorandum No. 33-77

The Jovian Environment

Laurence M. Trafton

GPO PRICE $ _____

OTS PRICE(S) $ _____

Hard copy (HC) __2.00__

Microfiche (MF) __.50__

jpl

JET PROPULSION LABORATORY
CALIFORNIA INSTITUTE OF TECHNOLOGY
PASADENA, CALIFORNIA
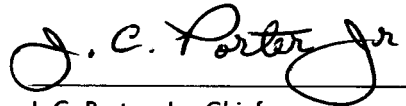
March 8, 1962

Technical Memorandum No. 33-77

The Jovian Environment

Laurence M. Trafton

J. C. Porter, Jr., Chief
Research Analysis

JET PROPULSION LABORATORY
CALIFORNIA INSTITUTE OF TECHNOLOGY
PASADENA, CALIFORNIA

March 8, 1962

CONTENTS

CONTENTS (Cont'd)

TABLES

FIGURES

ABSTRACT

24983

Our quantitative knowledge of the Jovian atmosphere and the environment above the atmosphere is summarized. The summary is based upon review and interpretation of the professional literature and will be revised as new observational and theoretical work is carried out at JPL and elsewhere. Topics covered include composition and structure of the atmosphere, photometric properties of the atmosphere, period of rotation, magnetic field, and the Jovian radiofrequency spectrum.

I. DEPTH OF THE ATMOSPHERE

The low mean density of Jupiter (1.35 g/cm³) has led to the conclusion that most of the mass of the planet is composed of hydrogen. Most of the heavier metals and silicates are presumably settled in a dense core, while the bulk of the interior and atmosphere is composed of light elements and compounds.

Jeffreys (Ref. 1) was the first to show that, by any reasonable hypothesis concerning the original temperature, the heat lost by a planet whose interior is in complete thermal communication with the surface is sufficient to solidify it. Hence, one expects a solid surface to exist on Jupiter. However, the opacity of the Jovian atmosphere is such that optical observation of this surface is impossible. Decameter radio waves (IXA) are capable of penetrating the Jovian atmosphere, and bursts in the 19-mc region are believed to arise from sources fixed on the planet. This fixed nature suggests a solid surface (Refs. 2, 3).

It was generally believed that the Jovian atmosphere must be very thick. However, in 1934, Wildt drew attention to the fast rate at which pressure must increase with depth to become sufficient to solidify the atmospheric gases or at least compress them to the density of the liquid state (Ref. 4). Peek (Ref. 5) suggested that this level lies only about 25 km below the visible surface. However, this value was based on too high a mean molecular weight of the atmosphere. Peek had assumed $\mu = 16$, whereas Baum and Code (Ref. 6) later found μ to be near 3 or 4, as discussed in Section IVA. As a result, Peek now agrees (Ref. 7) that the figure of 25 km may well be too small by a factor of 4 or 5. Assuming that the mean molecular weight does not vary appreciably with depth in the lower atmosphere, an atmospheric depth of about 100 km is implied. Peek chose a model (Refs. 5, 7) in which he assumed a law for the decrease in the lapse rate with depth and selected $\mu = 4$. From this, he deduced that the atmosphere would be com-

pressed to the density of solid hydrogen (6.08 g/cm³) at an effective depth of between 100 and 120 km. Thus, it is probable that the depth of the Jovian atmosphere is really very shallow compared with Jupiter's radius.

Wildt (Ref. 8) suggested that the depth of a hydrogen Jovian atmosphere (below 1 atm pressure) would be about 1% of Jupiter's optical radius; i.e., about 700 km. His calculation is based on a pure hydrogen and an isothermal atmosphere. The pressure of other gases will decrease this calculated distance considerably, whereas a temperature gradient acts to increase it. Pronounced effects of the latter are improbable, as only a subadiabatic temperature gradient should exist deep below the cloud level (see Sect. VIIIA-4). Thus, 700 km might be taken as an upper limit of the atmospheric depth.

The best model seems to be that of Peek (Refs. 5, 7), mentioned above, where $\mu = 4$ and a lapse rate was considered. Baum and Code's value of $\mu = 3.5$ is probably not off by more than 50% (see Sect. IVA). Hence, it is very likely that the depth of the Jovian atmosphere lies between 80 and 230 km below the upper surface of the cloud layer. More accurate knowledge of the temperature gradient is needed to specify the depth of the atmosphere more precisely. One result of these calculations is the indication that the mass of the Jovian atmosphere must be negligible compared with that of the solid planet (Table 1).

Table 1. Depth of the Jovian atmosphere

Depth[a] km	Source
700	Isothermal model (Ref. 8) pure hydrogen atmosphere. May be an upper limit.
230	
120[b]	Probable range set by uncertainty in mean molecular weight in
100[b]	Peek's model. $1.8 \leqq \mu \leqq 5.2$.
80	

[a]The depth for 700 km is that below a height at 1 atm pressure; the remaining values refer to depths below the cloud level.
[b]Likely range set by Peek's model for $\mu = 4$.

II. PERIOD OF ROTATION

A. Rotation of the Atmosphere

It was mentioned in Section I that the solid surface of Jupiter cannot be seen beneath the atmosphere. The apparent rotation of the planet is the over-all movement of its spotted and belted atmosphere. Observations of atmospheric features show that the Jovian atmosphere is rotating differentially, with the shortest period near the equator and the longest near the poles. There is also much non-uniformity or scatter in the periods of individual features, because they are continually moving with respect to each other in the fluid atmosphere.

By timing the transits of various spots visible in the atmosphere over many periods, it was noticed that the portion of the atmosphere at less than 10° latitude has a comparatively short period. This zone streams around the planet about 5 min faster than the regions in the high latitudes. The slower differential streaming which occurs at all latitudes is superimposed on this motion.

Two systems of longitude (Ref. 9) have been created to serve as reference for the atmosphere. System I has a rotation period of $9^h\ 50^m\ 30\overset{s}{.}003$ and is used as a reference frame for the class of objects in the fast-moving equatorial stream within 10° of the equator. System II, on the other hand, has a rotation period of the standard meridian of $9^h\ 55^m\ 40\overset{s}{.}632$. It is used as a reference for objects lying outside the equatorial stream, and its period is very close to that of the Great Red Spot between the oppositions of 1890 and 1891.

B. Period of the Solid Surface

1. Observations of Atmospheric Disturbances Occurring at the Same Latitude

One would expect violent disturbances on the solid surface of Jupiter to be manifest at the surface of the atmosphere in the form of local turbulence and mixing. If the atmosphere has a longitudinal motion with respect to the solid surface, these disturbances will spread out at a constant latitude. Suppose that at various time intervals a succession of disturbances is observed at a constant latitude and a succession of longitudes. If a longitude system, rotating beneath the clouds, can be found in which the longitudes at which the disturbance *first* occurred all prove to be the same, the period of the source of the disturbance is determined. This, presumably, is the period of the solid planet, especially if there is no differential variation in the period with latitude or if the results give small residuals over a long time interval. Accuracy de-

mands that the area of the source of the disturbance be small compared with the disk. Reese (Ref. 10) and Peek (Ref. 11) have described the results so obtained. In general, this method gives ambiguous results, because one is unsure of the identity of the sources. For this reason, it is difficult to decide between $9^h\ 55^m\ 42\overset{s}{.}66$ and $9^h\ 54^m\ 52\overset{s}{.}54$ or other periods in this range. The safest policy is to assume an uncertainty of about 50 sec in the period obtained by this means. If the individual sources can be identified through a better determination of the period by decameter waves, then Reese's method might improve this period (because of the long time lever) to give the highest accuracy of all. In addition, these sources on Jupiter would then be mapped.

2. Observations of Decameter Radio Emission

This method involves measuring the bursts of emission over the entire visible disk at decameter wavelength. Because of directional effects in emission, this disk is reduced to a size at which reasonably localized readings of longitude are obtained (see Sect. IXA). Readings are converted into probabilities of occurrence. When these are plotted in System I longitude, a general smear is obtained. However, when they are plotted in System II (over an interval of 100 days), the histograms show well defined maxima. This indicates that the radio source period lies close to that of System II. Carr *et al.* (Ref. 2) employed this method in early 1957 using 18.0-mc waves. Comparison with other work done in 1951 and 1955 increased the time lever to 5½ years. The results of this comparison show that the maxima exhibit a *uniform* and *parallel* shift in their longitudinal coordinates of System II. This means that the radio source is moving slowly and at a constant rate with respect to System II. The period of this radio source was found to be 11.8 sec shorter than that of System II; i.e., $9^h\ 55^m\ 28\overset{s}{.}8$.

An error of 10° in locating the maximum on the histograms will result in an error in this period of only about 0.2 sec. Replotting the probabilities vs longitude in this new system (System III*) noticeably sharpens the maxima on all three dates. Hence, System III is better than System II for plotting the radio sources.

There is evidence that the radio sources are anchored to the solid part of the planet. The three major sources

---

*System III coordinates were equal to those of System II on 0^h U.T., January 1, 1957.

tend to maintain their geographical configuration. There seems to be no pronounced differential effect on their position as there would be for three randomly located atmospheric sources. Observations through 1960 confirm this evidence (Ref. 3). Five sets of data spanning eight years show constancy of location of the principal noise source (Fig. 1).
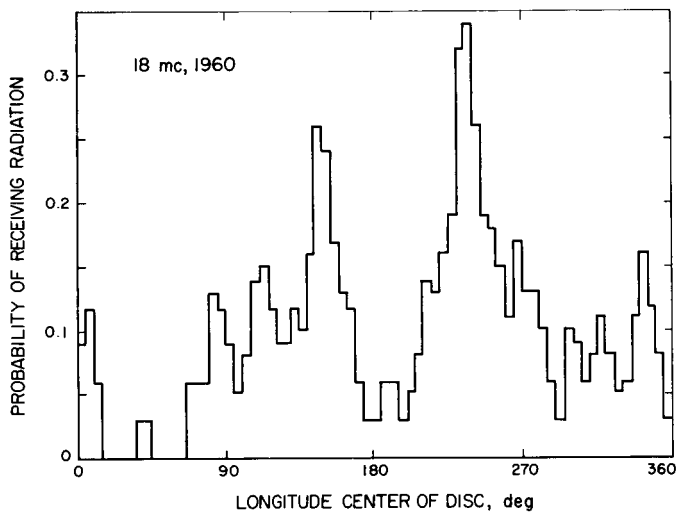
Fig. 1. Probability of receiving radiation from Jupiter vs longitude of center of visible disk (from Ref. 38 by permission from the publisher)

However, after plotting the 1959 and 1960 data, Carr et al. (Ref. 3) observed a slight residual shift, indicating that a refinement of their System III period was needed. A new analysis of the data was made (Fig. 2). In order to avoid residuals which might arise from possible shifting of the radio sources with frequency, it was decided to use only 18-mc data from all available records. This frequency was near the spectral maximum of the bursts (see Sect. IXA-1). The data employed were those obtained in 1951 by Shain (Ref. 12), in 1955 by Franklin and Burke (Ref. 13), and in 1957, 1958, 1959, and 1960 by Carr et al. (Refs. 2, 3). The corrected System III period was found to be $9^h 55^m 29\overset{s}{.}35$, which is very close to the value of $9^h 55^m 29\overset{s}{.}37$ derived independently by Douglas (Ref. 14) from a statistical analysis of the data of all previous workers. Gallet's (Ref. 15) result was $9^h 55^m 29\overset{s}{.}55$ $\pm 0\overset{s}{.}02$ for the System III period. However, this figure is derived from comparison of longitude profiles only from 1951 to 1957. The time lever is not as long as in the value of the period obtained by Carr et al., $9^h 55^m 29\overset{s}{.}35$. The given error in Gallet's period, $\pm 0\overset{s}{.}02$, seems rather small. It depends on the system of longitude used to plot the bursts. Using System II to analyze Shain's 1951 and 1956–1957 data, Gallet obtained a period of $9^h 55^m 29\overset{s}{.}70$
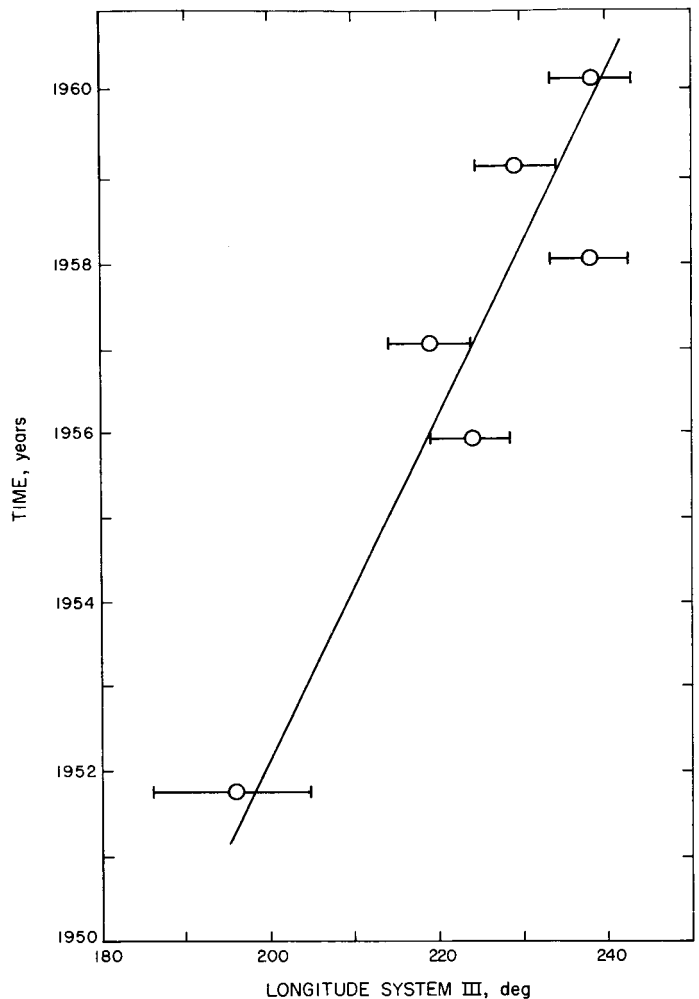
Fig. 2. Drift of center of principal Jupiter radio source A in original System III coordinates (from Ref. 3 by permission from the publisher)

$\pm 0\overset{s}{.}06$ for 18 mc. He performed the same analysis using his "Provisional System III," which coincides with System II at 0^h U.T., January 1, 1956 and has a period of $9^h 55^m 29\overset{s}{.}4$. This figure is very close to the Carr et al. period for System III. Gallet thus obtained the period $9^h 55^m 29\overset{s}{.}55$ $\pm 0\overset{s}{.}02$. These two determinations differ by $0\overset{s}{.}15$; this difference is probably due mainly to the difference in shape of the peaks and valleys in the longitude profiles for the two systems. (These peaks might arise from nonuniformity in the scatter of the radio bursts emitted over several months.) The determination based on System III periods is thus more reliable, because these periods are closer to the true period of the solid surface. Gallet also derives a period from his 1956–1957 data which is higher than that of 1951–1957 by 1.4 sec. The error of the 1956–1957 determination is given to be ± 0.25. However, Gallet combines the 18-mc and 20-mc data in this evaluation. Since the bandwidth of pulses is about 0.5 mc (Ref. 15),

these frequencies probably give independent bursts. Hence, these bursts could arise from separate sources of slightly different longitudes and thus yield a variable mean longitude, depending on relative outburst data. Gallet's best determination of the period of the solid surface is thus most likely to be $9^h\ 55^m\ 29\overset{s}{.}55$.

Carr *et al.* also used frequencies near 18 mc to avoid errors arising from the possibility that the centers of the radio sources shift with frequency (Ref. 3). The data, except for Shain's, were also independent of Gallet's data and extended over a large time span. The best value of Carr *et al.* is $9^h\ 55^m\ 29\overset{s}{.}35$.

3. Conclusion

In conclusion, it is decided that the sidereal rotation period of the solid surface of Jupiter lies in the range $9^h\ 55^m\ 29\overset{s}{.}45\ \pm0\overset{s}{.}10$, and the best determination so far is $9^h\ 55^m\ 29\overset{s}{.}35$.

Using this latter value to define the new System III period, the longitude of the central meridian at 0^h U.T. on Julian date J can be found from the published System II longitude (Ref. 9) for the same time by means of the relationship (Ref. 3)

$$\lambda\mathrm{III} = \lambda\mathrm{II} + 0.2747\,(J - 2{,}435{,}839.5)$$

III. PHOTOMETRIC MAGNITUDE, COLORS, AND ALBEDO

A. Magnitude of Jupiter

Because of the variable color patterns of the Jovian atmosphere, Jupiter's magnitude is variable. The magnitude in the visual region of the spectrum* is $V(1,0)$ at zero phase angle when Jupiter is at unit distance from the Sun and Earth; $V_0 = V(1,0) + 5 \log a(a-1)$ is the "mean opposition magnitude," where a is the semimajor axis of the planet's orbit. Harris (Ref. 6) quotes the mean of $V(1,0)$ over 23 oppositions: $V(1,0) = -9.25$, with individual oppositions varying from -9.03 to -9.48. The reduction to mean opposition is -6.70 mag; therefore, $V_0 = -2.55$ for Jupiter. There appears to be a long-range variability in $V(1,0)$, but insufficient data are available to draw any conclusions about its period. The magnitude also increases linearly with increasing phase angle by 0.1 to 0.4 mag over 12° (Ref. 16).

B. Colors of Jupiter

The U, B, V color system of Johnson and Morgan (Ref. 17) and the R, I color system of Hardie (Ref. 18) are adopted here. The zero point of the V magnitudes was fixed to agree with the IPv magnitudes of the north-polar sequence. The effective wavelengths for solar radiation are given as

U (ultraviolet) 0.353 μ
B (blue) 0.448 μ
V (visual) 0.554 μ
R (red) 0.690 μ
I (infrared) 0.820 μ

The colors of Jupiter are given with respect to those of the Sun. For the Sun, zero points defined by

$$U - B = 0.14$$
$$B - V = 0.63$$
$$V - R = 0.45$$
$$R - I = 0.29$$

are used, where V is taken as $V = -26.81$ and is uncertain by not more than ± 0.1 mag (Ref. 16).

Jupiter's colors are quoted by Harris (Ref. 16) from yet unpublished results of the McDonald measures of U, B, V and measures of R and I made by Hardie at the McDonald and Lowell Observatories. These measures give

$$U - B = +0.48$$
$$B - V = +0.83$$
$$V - R = +0.50$$
$$R - I = -0.03$$

*The effective wavelength of the V filter is $\lambda_{eff} = 0.554\ \mu$.

The corresponding differences, Jupiter–Sun, are given for ΔV taken to equal zero:

$$U = +0.54$$
$$B = +0.20$$
$$V = +0.00 \pm 0.04$$
$$R = -0.05$$
$$I = +0.27$$

Since these colors are based on broad-band filters, they are affected by differences in absorption bands. The colors are integrated over the disk of Jupiter and change with a net change of color as a result of variations in the belts and spots of its atmosphere. The error in the determination of magnitude for a given observation is about ± 0.02, but it has been seen that V changes by 0.45 over 26 observations (Sect. IIIA). However, color differences and colors whose V is set at $+0.00$ mag should not change by such a large value. The error should be about ± 0.04.

Kuiper (as discussed in Ref. 16) has measured intensities at 1 and 2μ using a lead sulfide photocell and broad-band filters. He obtained

$$\frac{I(2\mu)}{I(1\mu)} = 0.21$$

for Jupiter, where this ratio has been adjusted to unity for stars of spectral type close to that of the Sun. Absorption bands at 2 μ are responsible for this small value.

C. Albedo of Jupiter

The Bond albedo A is defined to be the ratio of flux reflected in all directions to the incident flux.

$$A = pq$$

where p is the "geometric albedo" and q is the phase integral

$$2 \int_0^\pi \phi(\alpha) \sin \alpha\, d\alpha$$

with $\phi(\alpha)$ being the ratio of the flux reflected at the planet at phase angle α to that reflected at phase angle zero. The geometric albedo can be measured from observations, but since the phase angle of light reaching the Earth from Jupiter never exceeds 12 deg, the phase integral must be inferred from theoretical considerations.

The geometric albedo p at the various colors for Jupiter is (Ref. 16):

$$p\,(U) = 0.27$$
$$p\,(B) = 0.37$$
$$p\,(V) = 0.45$$
$$p\,(R) = 0.47$$
$$p\,(I) = 0.35$$

The uncertainty is 5% in p. These values follow from the definition of p,

$$\log p = 0.4\,[m\,(\text{Sun}) - m\,(1,0)]$$
$$- 2 \log \frac{\text{mean radius}}{\text{Earth's mean radius}} + 8.741$$

where $m\,(1,0)$ is the magnitude of Jupiter at unit distance and zero phase in the color concerned. For the Sun, Harris' visual magnitude $V\,(\text{Sun}) = -26.81$ was adopted. An uncertainty of ± 0.05 mag in $V\,(\text{Sun})$ introduces an uncertainty of 5% in p. Twenty-six observations spread over a century (Sec. IIIA) showed $V\,(1,0)$ to vary 0.5 mag. Thus, the albedo may change slowly with time.

The phase integral q for a Lambert surface is 1.5. Harris (Ref. 16) has chosen $q = 1.65$ in the visual region. This gives a value of the Bond albedo in this visual region for Jupiter of

$$A_V = 0.73$$

This value replaces the previous one of 0.51 quoted by Kuiper and Harris (Ref. 19). Assuming optically thick atmospheres, Horak (Ref. 16) determined from limb-darkening measures that the particle phase function must have a forward component which decreases with wavelength, becoming nearly isotropic in the ultraviolet. He obtained a value of $q = 1.77$. Harris chose a less extreme particle-phase function which did not weight the darkening results near the limb as much and thus obtained $q = 1.65$ for the visual region. Harris' value for the Bond albedo in the visual region, $A_V = 0.73$, is probably representative of the true value. Because of different weighting in the particle phase function, Horak's and Harris' values of q differ by about 0.1. This error of about 7% in q, considered with the error of about 5% in p, would imply an error of about 12% in A_V. Hence, the visual Bond albedo (5540 Å) probably lies within the range $0.64 \leqq A_V \leqq 0.82$.

Rocket measurements (Ref. 20) at a height of 140 km in the upper atmosphere indicate a Jovian reflectivity of 0.26 at 2700Å effective wavelength. The uncertainty is $\pm 15\%$. A flux of 1.5×10^{-3} erg cm^{-2} sec^{-1} per 100 Å was measured. For λ^{-4} (Rayleigh) scattering, the derived fluxes would be 10% greater, which is within the uncertainty.

IV. OCCULTATION AND ECLIPSE RESULTS

A. Mean Molecular Weight

Baum and Code (Ref. 21) determined the mean molecular weight $\bar{\mu}$ of the upper Jovian atmosphere through the occultation of σ Arietis. They made the plausible assumptions of an isothermal stratosphere, an atmosphere of negligible thickness with respect to the planetary radius, and a constant value of gravity in the locality of the occultation. Assuming $g = 2600\,cgs$ and a temperature of $86°K$ for the stratosphere, they got a best fit for $\bar{\mu} = 3.3$. This value is unlikely to be wrong by more than 50%:

$$2 \leqq \bar{\mu} \leqq 5$$

The low value indicates that the bulk of the Jovian atmosphere is composed of hydrogen and helium. Eighty-percent extinction took 10 sec. If the atmosphere were composed primarily of methane, the next-lightest gas, the star would have lost 80% of its light in only 1 sec. Hence, there cannot be a dominance of any gas other than hydrogen or helium in the upper regions of the Jovian atmosphere.

B. Pressure Variation with Altitude

This variation can probably be approximated by the barometric formula

$$P_1 = P_2 \left[\exp - (h_1 - h_2)\frac{g\mu}{RT} \right]$$

where P_1 and P_2 are pressures at levels h_1 and h_2, respectively; and

$$g = 2600 \text{ cg}$$
$$T = 86°K \text{ (stratospheric temperature)}$$
$$R = 8 \times 10^7 \text{ (gas constant)}$$
$$\mu = 3.3 \text{ (mean molecular weight)}$$

Only relative pressures can be obtained in this manner. In Section VI, a value of about 0.4 ± 0.2 atm is derived for the pressure at the cloud level. This value is close to that of Kuiper's second model of the upper Jovian atmosphere (Ref. 19). Kuiper assumed abundance ratios $H_2 : He : CH_4$ to be the same for Jupiter as for Uranus and Neptune. He determined these ratios for the latter planets by evaluating a parameter which roughly takes into account the change in abundance ratios from the initial to the present composition of the gaseous envelope. The observed Jovian CH_4 abundance then yields 21 km-atm of H_2 and 32 km-atm of He. These values suggest a pressure of 2 atm at the cloud level. Kuiper's second model also indicates that the top of the cloud layer is about 21 km below the tropopause. This model should

be correct within an order of magnitude, judging from a comparison of pressures at the cloud level indicated by the model and computed in Section VI. This may mean that the region just above the clouds deviates from isothermalcy, and the above expression is valid only in the stratosphere. Below the clouds, the pressure variation depends on the temperature gradient. In any case, the pressure must increase very rapidly with depth (Ref. 1).

The average molecular weight of Jupiter's upper atmosphere is about seven times less than that of the Earth. On the other hand, its temperature is about half and its surface gravity 2.65 times that of the Earth. Hence, the percentage change of density or pressure from one level to another in Jupiter's atmosphere is similar to that in the Earth's atmosphere.

C. Atmospheric Absorption and Refraction

Eropkin (Ref. 22) measured photographically the extinction of Sunlight due to the non-transparency of the Jovian atmosphere. Observations were made of the decrease in intensity of the Jovian satellites during eclipse. The difference between this integrated intensity curve and the theoretical curve for a transparent atmosphere ranges from 3.2 to 3.7 min. If this difference is called q and the half-period of the transit of a satellite is called p, then the total extinction Q in units of the light falling on the Jovian disk πr^2 is

$$\underset{\sim}{Q} = \frac{\pi r^2 \left(1 + \frac{q}{p} \right)^2 - \pi r^2}{\pi r^2} \sim 2\frac{q}{p}$$

$$\underset{\sim}{Q} = 0.09 \pm 0.02$$

Thus, the extinction in the Jovian atmosphere amounts to about 9% of the entire amount of light falling on Jupiter's disk.

Eropkin's eclipse curves (Ref. 22) show a decrease in brightness amounting to 30–40% several minutes before the eclipse. Link (Ref. 23) suggested that the decrease represented the presence of an absorbing layer very high in Jupiter's atmosphere. However, this large pre-eclipse decrease is not manifested in the Harvard visual observations, in King's photographic observations, nor in any of Harris' photographic light curves, although he made a special effort to discover any such peculiarity. Such a decrease in intensity could not exceed 0.2% (Ref. 16).

Baum and Code (Ref. 21) have shown that differential refraction, rather than absorption, is the principal attenuating factor in the upper Jovian atmosphere. When refraction is allowed for, the light curve of the eclipse does not "terminate"; rather, it decreases asymptotically to zero as 1/time (Ref. 16). Kuiper's visual observations note such a "halt" in the light curves near 14 mag, lasting 1–2 min. With the 82-in. telescope, the eye can follow the eclipse to intensities fainter than the 0.2% set by the bright background on the photocell. Hence, it appears that Kuiper's observations can be explained by the effects of refraction.

V. COMPOSITION OF THE ATMOSPHERE

A. Methane Abundance

Kuiper (Ref. 19) made laboratory comparisons with planetary spectra to compile his Provisional Table of Atmospheric Compositions. A grating spectrograph of 50-Å/mm dispersion was employed in the methane-abundance determination using the band at 0.6–0.9 μ. An average path length of 2 air masses was assumed, since the atmosphere is optically thick. Kuiper thus obtained 150 m-atm of methane above the cloud level of Jupiter.

This result is approximate, because both temperature and pressure affect the shape and intensity of a band and because an adequate theory of line formation does not exist in an optically thick atmosphere. Comparison with a laboratory source near these correct values would have to be made for greater accuracy. If the accuracy is the same as in the ammonia determination, the true value should lie within ±50 m-atm of this value.

B. Ammonia Abundance

Dunham (Ref. 24) considered it probable that the total amount of ammonia vapor above the unit area of the reflecting layer on Jupiter corresponds to approximately 5–10 m of the gas under standard conditions. The vapor pressure required to support this mass implies a temperature of about 150°K if hydrogen is in great excess. This is in agreement with the radiometric temperature of 140 ± 10 deg and is well below the freezing point of ammonia; hence, the observed vapor must be in equilibrium with the solid ammonia crystals. The vapor pressure is then a function of temperature only.

Kuiper (Ref. 19), in agreement with Dunham, obtained 7 m-atm of ammonia above the cloud level. This value is probably good to ±2 m-atm.

C. Hydrogen Abundance

Zabriskie (Ref. 25) reported that the atmosphere of Jupiter has 5.5 km-atm of hydrogen above the cloud level. It is unlikely that this abundance is below 4 or above 6 km-atm of H_2 above the clouds (Ref. 26). Zabriskie derived these values from the (3-0) quadrupole lines of hydrogen found in the spectrum of Jupiter by Kiess, Corliss, and Kiess (Ref. 27). Equivalent widths were estimated by comparison with known solar lines, giving 0.08 and 0.04 Å for the S(1) and S(0) lines, respectively; the latter value was uncertain.

At first sight, it may seem that Zabriskie's value is rather low. Kuiper's second model predicts 21 km-atm of H_2 above the clouds (Sect. IVB). In addition, one would expect Jupiter to retain more hydrogen than Uranus or Neptune. Herzberg (Ref. 28) obtained 8 km-atm of H_2 above the clouds of Uranus and Neptune from compari-

son of the pressure-broadened 8270-Å quadrupole feature of hydrogen with a laboratory sample at 78°K and 100-atm pressure. This feature has not been observed on Jupiter. The estimated amount of methane is also greater for Uranus and Neptune than for Jupiter: 3 km-atm vs 0.15 km-atm, respectively (Ref. 19).

It must be remembered that these values refer to abundances *above the cloud level.* The measured ammonia abundance is 7 m-atm for Jupiter but is not detectable on Uranus or Neptune because of the very low vapor pressure occasioned by the low temperatures of these planets. One is thus able to see further down into the atmospheres of Uranus and Neptune, and hence, the higher measured abundances of H_2 and CH_4 are explained. It appears that the cloud layer on Jupiter is very high. There may well be more hydrogen on Jupiter than on Uranus or Neptune when the entire atmospheres are considered.

Kuiper's second model gives large abundance, because it overestimates the abundance ratios $H_2:He:CH_4$. When Kuiper's analysis for the composition of his second model is applied to Herzberg's data on Uranus and Neptune, one obtains (Ref. 19) for these planets:

$$135 \text{ km-atm of } H_2$$

$$373 \text{ km-atm of He}$$

$$3 \text{ km-atm of } CH_4$$

Assuming the same ratios for Jupiter, one obtains 6.8 km-atm of H_2, which is in closer agreement with Zabriskie.

Kiess, Corliss, and Kiess' plates show superior resolution in comparison with Dunham's plates (Ref. 24). Identified are 30 NH_3 lines in the $\lambda 6450$ band in Dunham's plates and 50 in those of Kiess *et al.* In the $\lambda 7920$ region, Kiess *et al.* measure about 140 lines and identify 110 vs Dunham's 39. Both observers used similar dispersions in the red. Kiess' plates were thus able to resolve the $Q(1)$, $S(0)$, $S(1)$, and $S(2)$ lines of the (3-0) transition, thereby identifying H_2 spectroscopically in Jupiter. These lines agree to ±0.04 Å with the laboratory lines; thus, it does not seem likely that the wrong lines were measured. Herzberg (Ref. 29) stated that the minimum layer for detection of the (3-0) quadrupole lines of H_2 is about 13 km-atm but that this may be accurate only within a factor of ten. The actual value will depend on the spectroscope and dispersion used. Hence, this Report does not necessarily contradict the value of 5.5 km-atm measured by Zabriskie from Kiess' plates.

D. Helium Abundance

Helium has not been detected or measured in the Jovian atmosphere. However, there are some inferences one can draw from analogy with Uranus and Neptune.

Herzberg (Ref. 28) observed three lines of the double transition (2-0), (1-0) in a laboratory spectrum of hydrogen, of which only the 8166-Å line was not hidden by strong methane absorption in the planetary spectra of Uranus and Neptune.

A double transition arises in the (3-0) band when the (1-0) transition takes place in one collision partner and the (2-0) transition in the other. This produces more spectral lines and gives rise to "odd" intensity ratios. The double transition is stronger than the single transition for pure H_2 at 78°K in the laboratory. Just the opposite is observed on Uranus: The 8166-Å line of the double transition is fainter than the single-transition 8270-Å feature.

The weakness of the planetary double transitions with respect to the single ones probably means that the hydrogen is strongly diluted with helium or nitrogen, so that most collisions suffered by the H_2 molecule are with a partner other than H_2. Experiments carried out using 3:1 and 9:1 helium to hydrogen mixtures show this strengthening of the single-transition band compared to the double-transition band but with a smaller effect, because helium atoms are not such efficient collision partners as hydrogen molecules in inducing the single-transition band. The 3:1 ratio may be favored by spectral comparisons for a temperature less than about 78°K.

Nitrogen is more active in inducing the single transition, but its abundance would have to be comparable with that of the hydrogen (Ref. 30). A comparable abundance would give a mean molecular weight near 15. In the case of Jupiter, such quantities of nitrogen are inconsistent with the measured mean molecular weight, which is between 2 and 5 (Sect. IVA).

If we make the assumption that the ratio $He:H_2$ is about the same for Jupiter, Uranus, and Neptune, then there should be roughly three times as much helium as hydrogen in the Jovian atmosphere. This figure is at best approximate; it is little better than an order of magnitude. However, it should not be too large, or the fractionation will be difficult to explain. The ratio 3:1 implies a mean molecular weight of 3.6 for the Jovian atmosphere.

VI. PRESSURE AT THE CLOUD LEVEL

Kuiper's second model (Ref. 19) assumed H_2, He, and CH_4 abundance ratios as derived for Uranus. However, the cloud layer is much higher in the case of Jupiter because of the increased turbulence and vapor pressure of ammonia. The stronger ammonia absorption obscures more hydrogen and methane. Assuming that the measured abundances are those above the cloud level of Jupiter, the pressure at this level can be guessed:

	NTP density g/cm³	Jovian abundance km-atm
H_2	8.9×10^{-5}	5.5
He	17.8×10^{-5}	16.5
CH_4	71.4×10^{-5}	0.15
NH_3	75.9×10^{-5}	0.007

The partial pressures are given by the product of density and length of tube containing the gas at standard temperature and pressure. An abundance of helium equal in volume to three times that of hydrogen is assumed. Abundances from Section V are assumed:

	Partial pressure, g/cm²	Partial pressure, atm
H_2	49	0.048
He	294	0.285
CH_4	10.7	0.010
NH_3	0.5	0.001
		0.35

The pressure at the cloud layer is thus about 0.4 atm, as indicated by present abundances. This value depends mainly on the assumed helium abundance. It is not likely that the true pressure exceeds 2 atm at the cloud level. An error of a factor of two in the helium abundance of the Jovian atmosphere results in a change in total pressure of 0.2 atm.

VII. RESULTS OF MEASUREMENTS OVER THE DISK

A. Limb Darkening

Let light of intensity I leave the planet in the direction of a distant observer. The position on the planet at which this ray originates is referred to by the angle $\theta = \cos^{-1} \mu$, as shown in Fig. 3. This enables one to measure the intensity variation with angle of emission and thus determine certain properties of the atmosphere.

In a linear expansion of $I(\mu)$ about the point $1 - \mu$,

$$I(\mu) = I(1.0)[1 - b(1 - \mu)]$$

Plaetscke and Barabashev's (Ref. 31) measurements give a value for $b = 0.9$ in the ultraviolet and 1.2 in the red region of the spectrum. According to Van de Hulst (Ref. 32), the accuracy of these results was probably overestimated. Kuiper (Ref. 32) found $b = 0.48$ at $\lambda 3500$ Å and $b = 1$ at $\lambda\lambda 8000$, 13,000, and 16,000 Å:

$$I(\mu) = I(1)[1 - 0.48(1 - \mu)] \quad \text{(ultraviolet)}$$

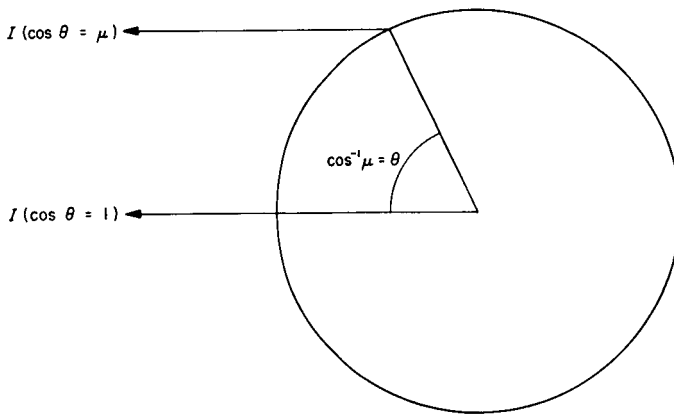$$I(\mu) = I(1)[1 - 1.0(1 - \mu)] \quad \text{(infrared)}$$

Fig. 3. Planetary geometry

Kuiper's values can be explained on the basis of the assumption that Jupiter's cloud surface approximately follows Lambert's law ($b = 1$) and that the atmosphere above the clouds is very thin. This is not in contradiction with the results of Section V.

A value of b higher than 1 might arise either from deviation from Lambert's law or from real absorption in the atmosphere. The latest determination, and probably the best, assumes a quadratic expansion of $I(\mu)$ in powers of $(1 - \mu)$ valid for $0 \leqq \mu \leqq 1$:

$$I(\mu) = I(1.0) [1 - b(1 - \mu) + c(1 - \mu)^2]$$

It is very difficult to obtain reliable observations of $I(\mu)$ for μ in the range $0 \leqq \mu \leqq 0.4$. Therefore, it is very difficult to determine both b and c from observations. Instead, consider the intensity at the "characteristic point," $\mu = 0.5$ or 0.866 of the distance from the center to the edge of the apparent disk, and define the ratio X (Table 2):

$$X = \frac{2I(0.5)}{I(1.0)} = 2 - b + \tfrac{1}{2}c$$

This ratio has the important property that, to the extent that $I(\mu)$ can be represented by a second-degree expansion, the geometric albedo (III C) is equal to

Table 2. Values of $X = 2 - b + \frac{1}{2}c$ vs λ for limb darkening

X	Spectral region	Source	Assumed limb darkening
1.52	Ultraviolet, 3,500 Å	Ref. 32	Linear
1.52	Ultraviolet	Ref. 16	Quadratic
1.01	Visual	Ref. 16	Quadratic
1	Red, 8,000 Å	Ref. 32	Linear
1	Infrared, 13,000 Å	Ref. 32	Linear
1	16,000 Å	Ref. 32	Linear

$$p = \tfrac{1}{3} I(1.0)(1 + 2X)$$

Measures of p in the ultraviolet region give $p(U) = 0.25$, leading to $X = 1.52$, in agreement with Kuiper's value for b, assuming that c is negligible (Ref. 16). This result alone could be interpreted as being due to isotropic scattering with albedo $\tilde{\omega}_0 = 0.85$. However, according to Harris (Ref. 16), isotropic scattering cannot explain the results in the blue, visual, and red regions, as the computed values of X are too large for the corresponding values of the geometric albedo p. In order to obtain agreement with the observed measures, it appears that one must postulate a forward-scattering particle phase function, such as $f(\cos \theta) = \tilde{\omega}_0(1 + a \cos \theta)$. Harris found $\tilde{\omega}_0 = 0.98$ and $a = 0.6$, for which $p = 0.43$ and $X = 1.01$, to explain the observations of Jupiter and Saturn in the visual region (Ref. 16). Limited accuracy of observations does not warrant use of a more complicated scattering function. This analysis is the basis for the upward revision of the Bond albedo, 0.73 (III C).

B. Band Absorption

Knuckles (Ref. 19), using medium dispersion spectra, reported that the $\lambda 6475$ NH$_3$ band, when compared with the solar group at $\lambda 6496$, varies in time. In a week or two, it may change in intensity by a factor of two. He further noted that while the Jovian polar region, on the whole, shows somewhat weaker absorption than the center of the disk (by a factor of 1.5), methane band strength appears constant over the disk.

In 1953, Hess (Ref. 33) reported surprisingly small center-to-limb variation in the strengths of NH$_3$ and CH$_4$ bands. The strength of absorption of NH$_3$ at 6441 Å and CH$_4$ at 6190 Å on Jupiter was seen to decrease slightly, rather than increase, toward the limb. Near the limb, the atmosphere is seen through obliquely, and hence, light should traverse a much longer absorbing path than it does near the center of the disk, where the path through the atmosphere to the cloud layer is minimal. This picture implies that greater absorption should be observed toward the limb.

The picture must be modified in light of these measurements. The observations made at $\pm 60°$ of longitude and latitude of the disk would have indicated a path length double that at the center of the disk. The methane above the clouds should all be gaseous at the temperature of Jupiter. The ammonia should be in equilibrium with its solid state, and hence, the amount of vapor, governed by the vapor pressure, should be a function of tem-

perature. On the other hand, the amount of methane found above a given point is a measure of the depth of that point.

There are now three ways in which Hess' observations might be explained:

1. The cloud surface of Jupiter rises toward the limbs, at least in the region within 60° of the center of the disk. Hess computes the cloud layer to be 10–12 km higher at ±60° longitude than at 0°. This would be interpreted to mean that the mid-day heat of the Sun evaporates the upper strata of the cloud layer. The higher level at ±60° obscures enough methane to account for the constant absorption over the disk.

   Hess finds that the NH_3 bands are slightly weaker at high latitudes than at the equator and much weaker near the morning limb. They are, however, nearly as strong at the evening limb as at the subsolar point. The temperature at the cloud level is connected with the amount of ammonia observed through the vapor pressure at the cloud level. Hess thus computes a temperature decrease toward the poles of about 6°K between the equator and latitude ±60°. The morning limb is calculated to be 4–5° cooler than the evening limb at ±60° longitude on the equator. He finds the morning limb to be 8–10 and the evening limb 4–9°K lower in temperature than the central meridian (Ref. 33).

2. The cloud surface is actually level, and the relative uniformity of methane absorption on Jupiter occurs, because the absorption falls on that portion of the curve of growth which lies between the linear and the square-root absorption regions (Ref. 33). In this region, the slope of the curve of growth is nearly zero, so that an increase of methane in the path would produce little or no increase in absorption. Hence, the constancy of methane absorption over the disk would be explained.

3. The cloud layer is actually level but is diffused by a covering layer of tenuous fog in the atmosphere (Ref. 30). In other words, we see about as deep into the atmosphere in one direction as in another. The cloud level has faded into the background at the subsolar point. Hence, absorption would be measured to be constant over the disk.

Hess gave two possible objections to observation 2. One is that the absorption is not exactly uniform, a slight decrease of absorption toward the limb taking place

rather than the slight increase implied by the region of the curve of growth. The second objection is that this region of the curve is reached only after a line has become saturated; that is, becomes rather dark at the center. The 6190-Å band of Jupiter's spectrum has 16.6% absorption. This band consists of 14 superimposed bands and, hence, is probably unresolvable. This implies that the composite band departs from complete absorption, because the lines composing it are unsaturated, not because the spectrograph integrates saturated lines with the adjacent continuum. It appears that the methane lines are not saturated. This suggests that observation 2 may not hold.

If the cloud surface is diffused, the temperatures determined by Hess are those of the effective level of penetration of the light rather than of the cloud surface proper. However, the altitude difference supposed by Hess to be that of the cloud level was based on half the measured path of methane being at ±60° and so corresponds to an effective level of penetration by 6190-Å light rather than of the cloud level.

C. Polarization Measurements

Lyot's polarization measurements (Ref. 34) neither contradict nor confirm those of Hess. His observations of the north and south polar regions extended to a latitude of 30° from the pole. He found that the polar regions may be covered by a fairly thick atmosphere in which Rayleigh scattering takes place. At the east and west equatorial limbs, he obtained values of the polarization $p = 0.0024$ and 0.0032, respectively (Ref. 19). Both the sign and the order of magnitude are different than in the polar regions. We have to assume that the atmosphere in the equatorial limbs is not very thick (Ref. 32). A thick atmosphere implies illumination of the atmosphere by the atmosphere; but a thin atmosphere is illuminated by the "bottom surface." It follows qualitatively that in the first case a negative, and in the second, a positive polarization results (Ref. 32). The extent of the visual grey regions and the sign of the polarization seem to coincide. This supports the view that the cloud level drops very rapidly in the polar regions as compared with the equatorial limb.

Dollfus (Ref. 30) was unable to confirm Hess' results and found that his polarization measurements can be explained by a tenuous fog. However, he confirmed Lyot's results by finding that the polar regions appear to be free of clouds, as the light scattered is polarized as expected for a pure gas.

Dollfus noted that over a central area, the polarization on the Jovian disk remains uniform. This polarization was observed to decrease with phase, from -10^{-3} at 2 deg phase to -6×10^{-3} at 12 deg phase (Ref. 35). Also, over a large central area, the polarization was not observed to be strongly dependent on wavelength. Its value at 11.7 deg of phase (maximum phase) lies within $-5.8 \times 10^{-3} \pm 1 \times 10^{-3}$.

Over the polar regions, Dollfus found the polarization to be independent of phase angle. The predominant vibration is always perpendicular to the limb. The value of the polarization is maximum at the pole and decreases to the value at the equator at a latitude which may be as low as 35°:

$P = 0.06$ to 0.08 at the poles

$P \simeq 0.02$ at 0.1 the distance from the limb of the disk to the center

$P = -0.007$ to 0 at 0.2 the distance from the limb of the disk to the center

Finally, Dollfus observed that the polarization increases toward the limb, depending on phase. The increase is least for maximum phase.

Hence, except for the polar regions, the polarization is dependent only on the phase angle and the distance to the center of the disk.

The above measurements are Dollfus' basis for the conclusion that a tenuous fog overlies the cloud layer on Jupiter. The previous model of an optically opaque cloud layer overlaid by a transparent gas contradicts the observations. The polarization of this model would increase rapidly with phase angle and would vary as λ^{-4}. As this is not the case with Jupiter, the atmosphere is assumed to be contaminated by a thin fog, whose polarization is of a sign opposite to that of a pure gas. Tables of scattering functions imply that particles of 1 μ diameter would behave in this way.

The fog must be thinner over the dark belts than over the bright zones and must disappear above the polar caps (Ref. 35). Thus, the cloud layer at the poles must be

very shallow indeed. Dollfus' conclusions are consistent with photographic records obtained in different spectral regions.

Urey (Ref. 30) objected to Hess' picture on the ground that the heat capacity of the Jovian atmosphere is probably too great to cause a change in temperature of 10°K at a given layer of the atmosphere in only 100 min (the time for a point in the layer to go from the subsolar point to longitude $-60°$ on the disk). In the presence of a thin fog, Hess' temperatures would refer to different effective layers, depending on the effective depth and angle of penetration of the observed light. It is more likely that the observed temperature difference is due to deviations from isothermalcy in the lower part of the visible Jovian atmosphere rather than to secular changes at a given level implied by an atmosphere whose cloud level depends on the apparent position of the Sun. Much of the Sun's energy will go into the heat of condensation of frozen ammonia particles before the temperature will rise, causing a decrease in the height of the cloud level.

D. Conclusion

In conclusion, combined polarization and absorption measurements indicate that a tenuous fog exists near the upper cloud layer; as a result, the cloud layer may be relatively level. This effect, however, does not seem to explain the higher temperature of 4–5°K found for the evening limb with respect to the morning limb. If real, this difference suggests that the cloud level does indeed vary in elevation. Urey's objection would be overcome if secular changes in temperature near the cloud level were very small. A temperature gradient of about 0.8°K/km would then correspond to Hess' results if the fog absorbed negligibly. Zabriskie (Ref. 25) found that the temperature at the cloud level is about 170°K, and possibly as high as 200°K. This is close to the melting point of ammonia, 195°K. The depression of the cloud level in the center of the disk would be explained as being due to the sublimation or melting of ammonia crystals by the Sun's heat near the subsolar region of the disk.

VIII. TEMPERATURES AND ENERGY BALANCE

A. Temperatures

1. Radiation Temperature

The maximum radiation temperature is the temperature at the subsolar point on a nonconducting, nonrotating body, at the mean distance of the given body from the Sun, with albedo equal to the visual albedo. The maximum radiation temperature of Jupiter is 120°K.

The mean radiation temperature of Jupiter is 85°K. To derive this temperature, it is assumed that the body receives radiation upon an area πR^2 but radiates from an area $4\pi R^2$ as a result of its rotation.

These theoretical figures are approximate. Their low values are a result of the high visual albedo and the assumption that the albedo in the infrared is zero. On the basis of the accuracy of the value for the visual albedo only, the uncertainty in these temperatures is 9%.

2. Radiometric Temperature

The radiometric temperature is the temperature obtained from water cell transmission in the 9–13 μ region (Ref. 36). For an assumed emissivity, this gives a temperature for Jupiter of 140±10°K, using the value 0.73 for the albedo (III C). This is the "gray-body" temperature at the effective level of formation of 9–13 μ radiation.

3. Temperature at the Cloud Level

The temperature at the top of the cloud layer was determined by Zabriskie (Ref. 25) to be 170°K or higher; possibly as high as 200°K. Kuiper (Ref. 19) chose two models of quite different H_2:He:CH_4 ratios and obtained temperatures of 168 and 165°K, quite insensitive to the composition of H_2 and He, using the 6450-Å ammonia band, the strength of which is quite sensitive to temperature on Jupiter. These temperatures refer to an effective level of penetration of light from the 6450-Å region in the Jovian atmosphere.

4. Temperature Variation with Depth

It is assumed that the temperature in the stratosphere is constant. It is given as about $2^{-\frac{1}{4}}$ times the mean radiation temperature, since the Gold–Humphreys theory should approximately apply to Jupiter's atmosphere, which contains CH_4 and possibly other polyatomic molecules (Ref. 19). This yields a temperature of roughly 71°K; and it may be higher (Sect. VIIIA-1). The temperature starts to increase with depth at the tropopause and has an unknown form below the cloud level. Wildt (Ref. 8) stated: "An *adiabatic* temperature gradient persisting over any *large* depth below the cloud level is clearly impossible because high temperatures would be reached very soon. Methane would then be destroyed irreversibly, and convective exchange with the atmosphere above the clouds would long ago have deprived it of all methane, which is so prominent a spectroscopic feature of·all the giant planets. There remains the possibility of a sub-adiabatic temperature gradient extending to great depths."

B. Energy Balance

Since only a very minor portion of Jupiter's thermal-emission spectrum has been observed (from 8 to 14 μ, 44 μ, and 3 to 4 cm), and since these regions are not representative, no accurate conclusion can be drawn as to the present magnitude of the heat flux from the interior.

If Jupiter's surface temperature is greater than 223°K, the peak of the black-body radiation is to the short wave-length side of 13 μ, and the "greenhouse effect" will really become effective (Ref. 37). Ammonia can radiate at low temperatures only in the region of 100 to 200 cm^{-1} and near 1000^{-1} cm, while the maximum black-body radiation at 105°K is 370 cm^{-1}. Since methane radiates only at higher frequencies than ammonia, no very effective infrared radiator is known to be in the higher atmosphere. Therefore, it is likely that the radiation from Jupiter originates at the deeper layers and is only partly absorbed by overlying colder layers (Ref. 36).

In the ultraviolet, Kiess *et al.* (Ref. 27) found a large tapering of the intensity with decreasing wavelength as compared with the spectrum of the Moon. The cause of this absorption is unknown.

Not much is known about the energy balance of Jupiter. The strongest absorbing molecule in the thermal region seems to be ammonia, but unknown species may be present. A weak line of methane has been detected at 44 μ (Refs. 19, 37). The abundance of methane may partly offset the small percentage of molecules in the upper state of this transition, so that radiation from the surface at this frequency would be inhibited. On the whole, fairly free radiation to space may occur, inhibited only by a few bands and an inefficient infrared scattering process (Ref. 37).
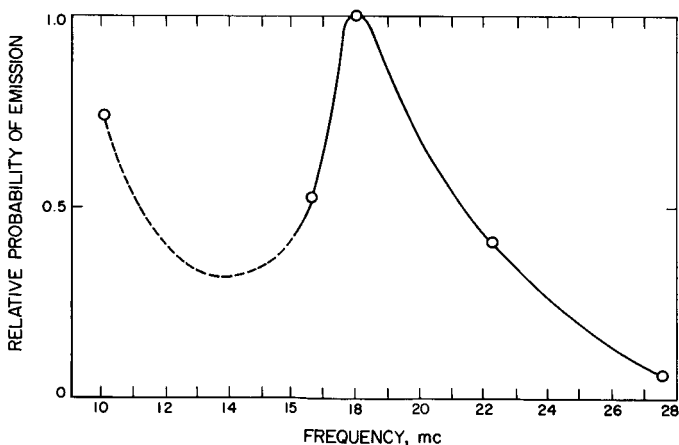
IX. RADIOFREQUENCY RADIATION

A. Decameter Waves

1. Spectrum

Most of the Jovian decameter radiation occurs in short bursts which fall in the frequency range of a few megacycles to 30 mc per second. The Earth's ionosphere filters out the lower-frequency waves, while there is an absence of Jovian emission at the higher-frequency side of the spectrum. The Earth's ionosphere also acts to reflect interference from distant thunderstorms and radio stations into the antennas.

The most active frequency lies between 18 and 19 mc and is detected about 10% of the observing time (Refs. 3, 38). The spectrum falls off remarkably with increasing frequency. An intense source at 22.2 mc occasionally reaches an intensity ten times that from the Crab nebula (Ref. 39). At the same time, a 38.7-mc interferometer having twice the gain of the 22.2-mc array failed to show any detectable trace of such a noise. The Crab nebula gave a trace having 15 times the background noise level. The tentative conclusion was that the maximum of the radio emission lies below 38 mc (Fig. 4).

Fig. 4. Relative probability of emission of radiation from Jupiter at various radiofrequencies

Subsequent observations have verified this conclusion. Only rarely has the emission extended to frequencies as high as 38 mc. It has already been stated that the maximum-occurrence frequency is near 18 mc (Ref. 3). This also appears to be the frequency of the most intense fluxes. In terms of the absolute energy received at the Earth's surface, the 19-mc bursts produce fluxes of as much as 10^{-19} w/m²/cps (Ref. 38), which is about 200 times as great as that from the most intense radio star.

The intensity of emission in the 18- to 27-mc region of the spectrum is also high. For 18.3 mc, Shain (Ref. 40) derived an intensity greater than 5×10^{-21} w/m²/cps (compatible with the previous value), while at 2.2 mc, Smith (Ref. 41) obtained a value of at least 2.2×10^{-22} w/m²/cps from Jupiter. Smith also reported that emission was not observed at 38 and 81.5 mc. This means that even if Jupiter does radiate here, the intensity of the emission must be less than 10^{-24} and 3×10^{-26} w/m²/cps, respectively.

Observations at 26.6 mc (Refs. 42, 43) made with an interferometer consisting of two corner reflectors each having 6 colinear halfwave dipoles as the active element yielded a peak power flux several times the strong Cassiopeia A source, corresponding to the order of 10 kw/cps bandwidth at Jupiter. This corresponds to about 10^{-21} w/m²/cps at the Earth. Table 3 summarizes these results.

Table 3. Comparison of fluxes at various frequencies

Frequency mc	Flux w/m²/cps	Source
18–19	10^{-19}	Ref. 38
18.3	$> .5 \times 10^{-20}$	Ref. 40
22	$> .2 \times 10^{-21}$	Ref. 41
26.6	10^{-21}	Refs. 42, 43
38	$< 10^{-24}$	Ref. 41
81.5	$< 3 \times 10^{-26}$	Ref. 41

Expressing the relation between flux density I and frequency V in the form $I = V^{-n}$, the results up to 1958 indicate (Ref. 44) that the spectral index n is greater than 5 between 22 and 81.5 mc and greater than 5.5 between 22 and 38 mc.

2. Total Decameter Radiation Power

Gallet (Ref. 15) estimated the radio power output of Jupiter per unit surface to be 100 times that of the quiet Sun. The total radiated power for a black body at 150°K is about 7.2×10^{18} w for Jupiter, whereas the total average radio power is about 7×10^{11} w. Thus, on the average, radio emission is still an inconspicuous fraction of the thermal radiation.

3. Nature of the Bursts

The Jovian bursts tend to occur in "storms." They do not occur constantly or produce steady emission, as is the case with the decimeter radiation. There is little or no correlation between pulses separated by more than 1 or 2 mc. In fact, the correlation between channels generally becomes poor when the receiver frequencies differ by a few tenths of a megacycle. However, it appears that increased sensitivity may extend this correlation to 1-mc width (Ref. 3). Some pulses still have widths of 0.4 and 0.2 mc (Ref. 3). The effective bandwidth of the dynamic spectrum is thus close to 0.5 mc.

Pulses tend to occur in pairs and triplets as well as singly. Groupings occur in which millisecond pulses are separated by ¼ and ¼₀ sec (Ref. 44). However, most of the pulses are from about 0.2 to 2 sec in duration, while the bursts themselves may last only a few seconds or as much as a minute (Ref. 38).

There is only a general correlation between the appearance of bursts at different frequencies. Observations of the same event at two locations imply that the Earth's ionosphere produces a local scintillation having a period of about 30–40 sec, superimposed on a more rapid one which distorts individual pulses (Ref. 3). This is thought to be the primary cause of the lack of correlation in the appearance of the bursts at different frequencies. Frequency drifts on the order of a few megacycles per minute for the storms were common (Ref. 3).

Gallet (Ref. 15) estimated that, on the average, 0.3 pulses per second occur which can be detected. This number would be a lower limit for the Jovian activity.

The Jovian activity varies with time approximately in an inverse relation to the sunspot cycle (Ref. 3). The activity went through a minimum in 1959. Several more years must pass before the closeness of this correlation can be ascertained.

When the bursts are plotted in a histogram (see Sect. II), they show surprisingly sharp maxima. These maxima remain fixed with respect to one another, indicating that the sources of the Jovian decameter radiation are anchored to the solid surface. The most active surface source is visible only over 135° of longitude, while most of its emission at 18 mc is contained within 20° of longitude (see Fig. 1). This means that the radio bursts are strongly directional. The directionality was attributed to the presence of a Jovian ionosphere; however, Carr *et al.* (Ref. 3) showed that the peak widths become narrower as the frequency increases. This phenomenon is inconsistent with the hypothesis that the directional characteristic of

Jovian radio emission is imposed by a Jovian ionosphere. There is no great difference between the 1959 and 1960 peak widths at various frequencies (Ref. 3).

Gallet (Ref. 15) gave the value of the radiated power per pulse as about 100 kw/cps and the total radiated energy per strong pulse as 10^{11} j. These figures are orders of magnitude. However, at least 10^9 j/mc of bandwidth have been observed (Ref. 44).

4. Location of the Sources

Three principal sources are distinguished on Jupiter. Their longitudes seem to vary with frequency (Ref. 3), and nothing is known about their latitudes. The principal source is located at about $250\pm15°$ in System III longitude (Table 4). The second-largest source in System III is located at about $135\pm10°$, and the third at about $330\pm20°$.

Table 4. System III longitude of the 1960 principal source vs frequency

Frequency mc	1960 longitude of peak deg
10	267
16.7	251
18	249
20	241
22.2	236

5. Polarization of the Bursts

The decameter radiation from Jupiter is circularly or elliptically polarized about 95% in the right-handed sense (Refs. 3, 45). The polarization has the same sense when measured both in the northern and southern hemispheres, so that the Earth's ionosphere cannot be responsible for the polarization. This effect, therefore, originates on Jupiter and is good evidence that Jupiter has both an ionosphere and a magnetic field (Ref. 46).

The axial ratio exhibits a large random fluctuation (Ref. 3) which is probably due to ionospheric scintillation in the Earth's atmosphere. However, in almost all cases, it is negative. Tables 5 and 6 give values of the axial ratio as obtained by Carr *et al.* (Ref. 3).

6. Correlations With Visible Phenomena

Photoelectric observations of Jupiter in Hα and white light over three occasions of strong radio signals showed

Table 5. Polarization measurements of Carr et al. (Ref. 3)

Location	Date	No. of pulses	Polarization %	Axial ratio
Chile	1960	882	96	−0.34
Florida	1960	33	94	−0.10
Florida	1958	30	100	−0.53

Table 6. Axial ratios of Chile data averaged by activity zone

System III activity zone deg longitude	No. of pulses	Axial ratio	Standard deviation
90–180	223	−0.32	0.20
190–280	608	−0.36	0.17
280– 10	39	−0.24	0.26

Table 7. Observed disk temperatures vs wavelength

Wavelength	Disk temperature °K	Flux q in terms of T_d/λ^2 °K/cm²	Source
10 μ	140 ± 10		
3.03 cm	171 ± 20	19[a]	
3.15 cm	145 ± 18	15 ± 2	Ref. 48
3.17 cm	173 ± 20	17[a]	Ref. 47
3.36 cm	189 ± 20	15 ± 2, 17	Ref. 47
3.75 cm	(200) ± 200	15	Ref. 49
10.2 cm	640 ± 85	6 ± 2	Ref. 50
21 cm	2500 ± 450	5.7[a]	Ref. 51
22 cm	3000 ± 1700	7.5 ± 3	Ref. 52
31 cm	5500 ± 1500	5.7 ± 1.6	Ref. 53
32 cm	7500 ± 2500	15 ± 6	Ref. 51
68 cm	70,000 ± 30,000		Ref. 52

[a] Flux from Ref. 54.

no evidence of light pulses from the planet (Ref. 3). Thus, there is no support for the concept that decameter radiation may be stimulated by particle bombardment from the Sun. There is no known correlation between Jovian decameter emissions and visible features in the atmosphere of Jupiter.

B. Microwave Radiation

1. Spectrum

Microwave radiation has been measured from 3.03- to 68-cm wavelength. Since this region is well above the infrared, where most of the planet's thermal radiation is emitted, one would expect the flux to fall off as λ^{-2} for black-body (or thermal) emission. It must also be assumed that the temperature over the range of the depth of penetration of microwave radiation would change negligibly.

The flux observations are summed up in Table 7 and Fig. 5. The flux at about 3.2 cm is approximately 15×10^{-26} w/m²/cps at the telescope (Fig. 6). At 22 cm, it has dropped to about 6×10^{-26} w/m²/cps but increases with wavelength approximately as $\lambda^{+0.2}$ (Ref. 52). The minimum falls at about 7- to 8-cm wavelength (Ref. 55). This suggests that the microwave emission below about 5-cm wavelength is primarily thermal, while that greater than 10 cm is primarily non-thermal (Ref. 56).

When the fluxes are converted into disk temperatures T_d of a black body subtending the same solid angle Ω as Jupiter by means of the relation $F_\lambda = 2K\Omega\,(T_d/\lambda^2)$, the disk temperature is seen to become implausibly high. Field (Ref. 56) shows that a hot atmosphere cannot account for the bulk of the microwave emission. Thus,

it does not seem that the temperature gradient below the clouds could rise fast enough to account for the increase in disk temperature with effective depth of penetration of the longer microwaves. Hence, the longer microwaves are nonthermal in character.

The temperatures in the thermal region of the microwave spectrum are close to the radiometric value, 140°K ±10. On the average, they are higher and increase with wavelength. This emission is interpreted as thermal emission from ammonia in the region near the top of the cloud layer (Ref. 47). The gaseous ammonia radiates through the inversion line at 1.28 cm, pressure-broadened by the presence of hydrogen and helium. Thermal radiation from lower levels in the atmosphere may compose a non-negligible fraction of the higher-temperature radiation at longer wavelengths in the centimeter and decameter region, although it cannot account for most of it.
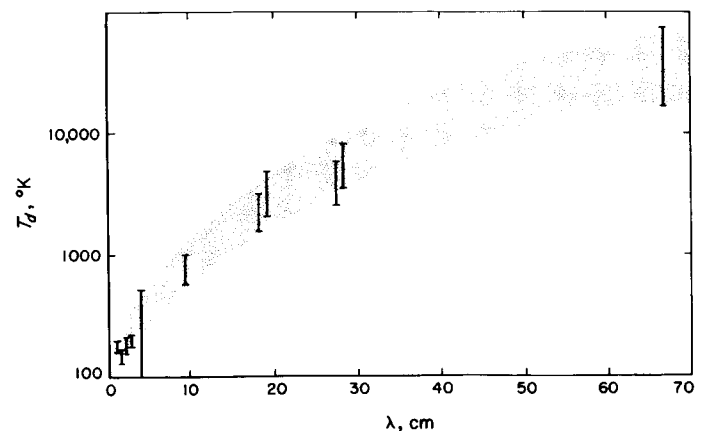
Fig. 5. Microwave spectrum of Jupiter vs equivalent black-body temperature
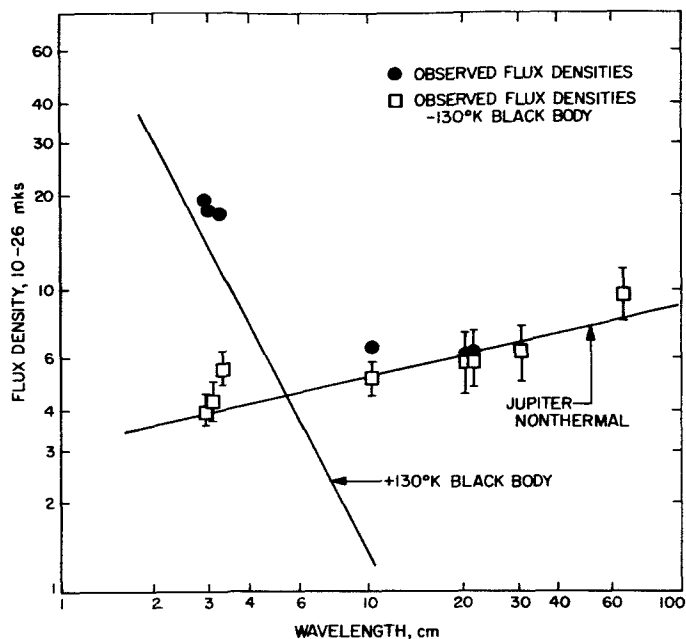
Fig. 6. Microwave spectrum of Jupiter vs flux density (from Ref. 55 by permission from the publisher)

2. Polarization—Jovian Van Allen Belt

The 31-cm radiation from Jupiter was found to be strongly linearly polarized in a direction nearly parallel to the equatorial plane (Ref. 57). The electric vector parallel to the equatorial plane is about 1.7 times as intense as in perpendicular polarization. No detectable pattern was observed when the antennae were cross-polarized in position angles of 0 and 90 deg. This implies the absence of any circularly polarized component greater than 6% of the radiation and that the vector of the linear component lies within $\pm 12°$ of Jupiter's equator. Observations with an antenna separation of 400 ft gave values for the degree of polarization between 25 and 43% for horns $\pm 45°$ from "north." For horns set "north" and "east," a mean polarization of 22% was obtained. These observations are consistent with an equatorial ring of mean diameter about 2 min of arc; that is, about three times the diameter of Jupiter. The maximum resolution was 2 min of arc, and the radiation thus measured coming from the outer part of this zone was observed to be more strongly polarized. It appears that 31-cm radiation is coming from the Jovian equivalent of a Van Allen Belt.

3. Secular Variation

At 3.15 cm, a disk temperature of 145°K ± 18 was measured (Ref. 48) in the 1957 opposition, while in 1959, a value of 173°K ± 20 was obtained (Ref. 47). The apparent increase is 1½ times the probable error.

In 1959, Sloanaker (Ref. 50) and McClain (Ref. 51) reported tentative periodic variations of 30% in temperature, roughly correlated with System II. Observations were at 10.3 and 21 cm, respectively. This effect was not observed at 31 cm. There may have been a local zone of increased emission near Jupiter's poles if this variation was real. Its period was 40 sec–2 min longer than that for System II—indicating high latitude for a source in the atmosphere.

However, Roberts and Stanley (Ref. 53) combined the observations of a number of sources and came to the conclusion that the variations were not significantly greater than those for the other weak sources. They found no significant correlation of these variations with System I or II longitude or with the Sacramento Peak Flare Index.

The value of the disk temperature at 10.3 cm seemed to drop by a factor of two from 1958 to 1959. The 1958 value is 640 ± 57, and the 1959 value is 315 ± 45 Ref. 58). The 1958 observation measured the electric vector at an angle of 67 deg with the equator, whereas in 1959, this angle became 79 deg. Radhakrishnan and Roberts' (Ref. 57) observations showed that it is necessary to consider the polarization of the antenna when evaluating the radio radiation received from Jupiter, because Jupiter's 31-cm radiation is almost completely plane-polarized. This difference in angle could account for the lower 1959 intensity. However, a very large polarized component of about 10 times the measured intensity would be required to account for the entire change in this way.

4. Source

Of the theories presented, only the Cyclotron and the Synchrotron theories can account for both the observed intensity and polarization (Refs. 56, 59). These models, however, imply either a very high magnetic field or an inexplicably high flux of energetic electrons.

The Cyclotron theory can account for the observed intensity (Ref. 57) if the electron density is similar to that in the Earth's Van Allen belt and a magnetic field of 300 gauss exists in the region of emission. This implies a field on the order of 10^4 gauss at the planet's surface. Field (Ref. 59) found that at least a 1200-gauss polar field must exist if the Cyclotron radiation from trapped electrons in a Van Allen-type belt is responsible for the emission.

Synchrotron radiation from relativistic electrons trapped in the Jovian magnetic field requires a very high particle density but can accommodate a much lower magnetic field. Relativistic electrons in a layer of depth $D = 10^{10}$

cm = 1.4 times Jupiter's radius in a field of 7 gauss, plus the condition that the brightness temperature equal the observed disk temperature at 31 cm, require that the number of electrons with energy greater than 1 Mev be about 10^{-2} per cm^3. This exceeds the estimated density in the Earth's Van Allen Belt by a factor of 3×10^4 (Ref. 53).

No observations of polarization and source size vs frequency have been published yet. Such observations may distinguish between the two mechanisms (Ref. 56).

No splitting of spectral lines due to a very large magnetic field has been observed.

X. THE JOVIAN MAGNETIC FIELD

A. From Decameter Waves

If, in addition to the measured axial ratio (Tables 5 and 6) of the polarization ellipse, the magnetic latitude of the sources and the critical frequency are known, the magnetic-field intensity on Jupiter can be calculated by means of the Appleton formula. Carr et al. (Ref. 46) made seemingly possible guesses of 20°S for the latitude and 17 mc for the critical frequency. The latter is deduced from the width of the active longitude sector and assumes that a Jovian ionosphere is responsible for limiting the direction of decameter waves. These assumptions lead to a value for the magnetic-field intensity in Jupiter's ionosphere of 7 gauss.

Later, Carr et al. (Ref. 3) found that the ionosphere probably is not the cause of the directional properties of

Jovian emission, because the widths of the histogram peaks decrease instead of increasing with frequency. This lends doubt to the validity of the 7-gauss value of the magnetic field.

B. From Decimeter Waves

Section IXB-4 states that if the decimeter radiation arises from a cyclotron process, at least a 1200-gauss—possibly a 10^4-gauss—magnetic field exists on the Jovian surface. If the Synchrotron process holds, the magnetic field could be low (e.g., 7 gauss), but then, the particle density of relativistic electrons must be on the order of 10^4 times that estimated in the Earth's Van Allen Belt.

REFERENCES

1. Jeffreys, H., "Constitution of the Four Outer Planets," *Royal Astronomical Society Monthly Notices,* Vol. 83, pp. 350–54, 1923.

2. Carr, T. D., A. G. Smith, R. Pepple, and C. H. Barrow, "18-Megacycle Observations of Jupiter in 1957," *Astrophysical Journal,* Vol. 127, pp. 274–83, 1961.

3. Carr, T. D., A. G. Smith, H. Bollhagen, N. F. Six, Jr., and N. E. Chatterton, "Recent Decameter-Wave-Length Observations of Jupiter, Saturn and Venus," *Astrophysical Journal,* Vol. 134, pp. 105–25, 1961.

4. Wildt, R., "Über die Stellardissoziation des Wasserstoffmoleküls," *Zeitschrift für Astrophysik,* Vol. 9, pp. 176–184, 1934.

5. Peek, B. M., "Physical State of Jupiter's Atmosphere," *Royal Astronomical Society Monthly Notices,* Vol. 97, pp. 574–82, 1937.

6. Baum, W. A., and A. D. Code, "Photometric Observations of the Occultation of σ Arietis by Jupiter," *Astronomical Journal,* Vol. 58, pp. 108–12, 1953.

7. Peek, B. M., *The Planet Jupiter,* Chapter 28, pp. 227–35. Faber and Faber, London, 1958.

8. Wildt, R., "Inside the Planets," *Publications of the Astronomical Society of the Pacific,* Vol. 70, No. 414, pp. 237–50, 1958.

9. U. S. Naval Observatory, *American Ephemeris and Nautical Almanac,* U. S. Government Printing Office, Washington. Published annually.

10. Reese, E. J., "Possible Clue to the Rotation Period of the Solid Nucleus of Jupiter," *British Astronomical Association Journal,* Vol. 63, pp. 219–21, 1953.

11. Peek, B. M., *The Planet Jupiter,* pp. 222–26. Faber and Faber, London, 1958.

12. Shain, C. A., "18.3 Mc/s Radiation From Jupiter," *Australian Journal of Physics,* Vol. 9, pp. 61–73, 1956.

13. Franklin, K. L., and B. F. Burke, "Radio Observations of the Planet Jupiter," *Journal of Geophysical Research,* Vol. 63, No. 4, pp. 807–24, 1958.

14. Douglas, J. N., "Uniform Statistical Analysis of Jovian Decameter Radiation, 1950–1960" (abstract only), *Astronomical Journal,* Vol. 65, pp. 487–88, 1960.

15. Gallet, R. M., "Radio Observation of Jupiter II," *Solar System,* Vol. 3, ed. by G. P. Kuiper and B. M. Middlehurst. Chapter 14, pp. 500–33, University of Chicago Press, Chicago, 1961.

16. Harris, D. L., "Photometry and Colorimetry of Planets and Satellites," *Solar System,* Vol. 3, ed. by G. P. Kuiper and B. M. Middlehurst. Chapter 8, pp. 272–86, University of Chicago Press, Chicago, 1961.

17. Johnson, H. L., and W. W. Morgan, "Fundamental Stellar Photometry for Standards of Spectral Type on the Revised System of the Yerkes Spectral Atlas," *Astrophysical Journal,* Vol. 117, No. 3, pp. 313–52, May 1953.

18. Hardie, R. H., Unpublished results.

19. Kuiper, G. P., "Survey of Planetary Atmospheres," *Atmospheres of the Earth and Planets,* ed. by G. P. Kuiper. Chapter 12, pp. 304–45, University of Chicago Press, Chicago, 1949.

20. Borgess, A., and L. Dunkelman, "Ultraviolet Reflectivities of Mars and Jupiter," *Astrophysical Journal,* Vol. 129, pp. 236–37, 1959.

21. Baum, W. A., and A. D. Code, "Photometric Observations of the Occultation of σ Arietis by Jupiter," *Astronomical Journal,* Vol. 58, pp. 108–12, 1953.

22. Eropkin, D. J., "Uber die Extinktion des Lichtes in der Jupiteratmosphäre," *Zeitschrift für Astrophysik,* Vol. 3, pp. 163–70, 1931.

23. Link, M. F., "Occultation et éclipses par les planètes," *Bulletin Astronomique, second series—Memoires et Varietés,* Vol. 9, pp. 227–49, 1933.

24. Dunham, T., "Atmospheres of Jupiter and Saturn," *Publications of the Astronomical Society of the Pacific,* Vol. 46, pp. 231–33, 1934.

25. Zabriskie, F. R. *Hydrogen Content of Jupiter's Atmosphere,* American Geophysical Union, 41st Annual Meeting, Washington, D. C., April 27–30, 1960.

26. Zabriskie, F. R., Private communication, 1961.

27. Kiess, C. C., C. H. Corliss, and H. K. Kiess, "High-Dispersion Spectra of Jupiter," *Astrophysical Journal,* Vol. 132, pp. 221–31, 1960.

28. Herzberg, G., "Spectroscopic Evidence of Molecular Hydrogen in the Atmospheres of Uranus and Neptune," *Astrophysical Journal,* Vol. 115, pp. 337–45, 1952.

29. Herzberg, G., "On the Possibility of Detecting Molecular Hydrogen and Nitrogen in Planetary and Stellar Atmospheres by Their Rotation-Vibration Spectra," *Astrophysical Journal,* Vol. 87, pp. 428–37, 1938.

30. Urey, H. C., "Atmospheres of the Planets," *Handbuch der Physik,* Vol. 50, ed. by S. Flügge. Pp. 363–415, Springer Verlag, Vienna, 1959.

31. Plaetscke, J., "Photographische Photometrie der Jupiterscheibe," *Zeitschrift für Astrophysik,* Vol. 19, pp. 69–115, 1939.

32. Van De Hulst, H. C., "Scattering in the Atmospheres of the Earth and the Planets," *Atmospheres of the Earth and Planets,* ed. by G. P. Kuiper. Chapter 3, pp. 49–111, University of Chicago Press, Chicago, 1949.

33. Hess, S. L., "Variations in Atmospheric Absorption Over the Disks of Jupiter and Saturn," *Astrophysical Journal,* Vol. 118, pp. 151–60, 1953.

34. Lyot, B., "Recherches sur la polarisation de la lumière des planetes et de quelques substances terrestres," *Annales de l'Observatoire de Meudon,* No. 8, 1929.

35. Dollfus, A., "Polarization Studies of Planets: Jupiter," *Solar System,* Vol. 3, ed. by G. P. Kuiper and B. M. Middlehurst. Chapter 9, Part 4.6, pp. 391–94, University of Chicago Press, Chicago, 1961.

36. Menzel, D. H., W. W. Coblentz, and C. O. Lampland, "Planetary Temperatures Derived From Water-Cell Transmission," *Astrophysical Journal,* Vol. 63, pp. 177–87, 1926.

37. Newburn, R. L., Jr., "Exploration of Mercury, the Asteroids, the Major Planets and Their Satellite Systems, and Pluto," *Advances in Space Science and Technology,* Vol. 3, ed. by F. I. Ordway. Pp. 196–266, Academic Press, New York, 1961.

38. Smith, A. G., "Radio Spectrum of Jupiter," *Science,* Vol. 134, No. 3479, pp. 587–95, 1961.

39. Burke, B. F., and K. L. Franklin, "Observations of a Variable Radio Source Associated With the Planet Jupiter," *Journal of Geophysical Research,* Vol. 60, No. 2, pp. 213–217.

REFERENCES (Cont'd)

40. Shain, C. A., "18.3 Mc/s Radiation from Jupiter," *Australian Journal of Physics*, Vol. 9, pp. 61–73, 1956.

41. Smith, F. G., "Search for Radiation From Jupiter at 38 Mc/s and at 81.5 Mc/s," *Observatory*, Vol. 75, pp. 252–54, 1955.

42. Kraus, J. D., "Some Observations of the Impulsive Radio Signals From Jupiter," *Astronomical Journal*, Vol. 61, pp. 182–83, 1956.

43. "American Astronomers' Report," *Sky and Telescope*, Vol. 15, pp. 358–59, 1955–1956.

44. Zhelezniakov, V. V., "On the Theory of the Sporadic Radio Emission From Jupiter," *Soviet Astronomy—AJ*, Vol. 2, pp. 206–15, 1958.

45. Franklin, K. L., and Burke, B. F., "Radio Observations of Jupiter" (abstract only), *Astronomical Journal*, Vol. 61, p. 177, 1956.

46. Carr, T. D., "Radiofrequency Emission From the Planet Jupiter," *Astronomical Journal*, Vol. 64, pp. 39–41, 1959.

47. Giordmaine, J. A., L. E. Alsop, C. H. Townes, and C. H. Mayer, "Observations of Jupiter and Mars at 3-cm Wave Length" (abstract only), *Astronomical Journal*, Vol. 64, pp. 332–33, 1959.

48. Mayer, C. H., "Planetary Radiation at Centimeter Wave Lengths," *Astronomical Journal*, Vol. 64, pp. 43–45, 1959.

49. Drake, F. D., and H. I. Ewen, "Broad-Band Microwave Source Comparison Radiometer for Advanced Research in Radio Astronomy," *Proceedings of the Institute of Radio Engineers*, Vol. 46, pp. 53–60, 1958.

50. Sloanaker, R. M., "Apparent Temperature of Jupiter" (abstract only), *Astronomical Journal*, Vol. 64, p. 346, 1959.

51. McClain, E. F., "Test for Non-thermal Microwave Radiation From Jupiter at a Wave Length of 21 cm" (abstract only), *Astronomical Journal*, Vol. 64, pp. 339–40, 1959.

52. Drake, F. D., and Hvatum, S., "Non-thermal Microwave Radiation From Jupiter," *Astronomical Journal*, Vol. 64, pp. 329–30, 1959.

53. Roberts, J. A., and G. J. Stanley, "Radio Emission From Jupiter at a Wavelength of 31 Centimeters," *Publications of the Astronomical Society of the Pacific*, Vol. 71, pp. 485–96, 1959.

54. Mayer, C. H., "Radio Emission of the Moon and Planets," *Solar System*, Vol. 3, ed. by G. P. Kuiper and B. M. Middlehurst. Chapter 12, pp. 442–68, University of Chicago Press, Chicago, 1961.

55. Drake, F. D., "Radio Emission From the Planets," *Physics Today*, Vol. 14, pp. 30–34, 1961.

56. Field, G. B., "Source of Radiation From Jupiter at Decimeter Wavelengths," *Journal of Geophysical Research*, Vol. 64, pp. 1169–77, 1959.

57. Radhakrishnan, V., and J. A. Roberts, "Polarization and Angular Extent of the 960-Mc/sec Radiation From Jupiter," *Physical Review Letters*, Vol. 4, pp. 493–94, 1960.

58. Sloanaker, R. M., and J. W. Boland, "Observations of Jupiter at a Wave Length of 10 cm," *Astrophysical Journal*, Vol. 133, pp. 649–56, 1961.

59. Field, G. B., "Source of Radiation From Jupiter at Decimeter Wavelengths: 2 Cyclotron Radiation by Trapped Electrons," *Journal of Geophysical Research*, Vol. 65, pp. 1661–71, 1960.